Applied Thermal Engineering 248 (2024) 123224

Contents lists available at ScienceDirect

Applied Thermal Engineering

journal homepage: www.elsevier.com/locate/apthermeng

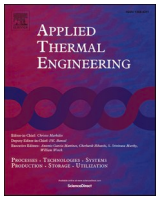

Research Paper

Design of adsorption chillers under rolling conditions in naval applications: Experimental and numerical approaches

Valeria Palomba [a,*], Antonino Bonanno [a], Vincenza Brancato [a], Andrea Frazzica [a], Ralph Herrmann [b]

[a] CNR ITAE, Salita S. Lucia sopra Contesse 5, 98126 Messina, Italy
[b] Fahrenheit GmbH, Siegfriedstr. 19, 80803 Munich, Germany

ARTICLE INFO

Keywords:
Adsorption chiller
Experimental testing
Waste heat recovery
Energy efficiency

ABSTRACT

International shipping is one of the major contributors to the overall greenhouse gases emissions and therefore its decarbonization is a key priority worldwide. Among the possible energy efficiency measures, the use of waste heat for cooling through adsorption chillers has gained significant attention. However, the proper integration of such kind of chillers on board needs to consider the effect of the rolling movement of the ship. In the present work, two different sorption modules (i.e the couple of adsorber + evaporator/condenser) are experimentally tested in horizonal position and at different inclinations, considering permanent tilting or continuous moving. The results were subsequently used for the implementation in a dynamic simulation model and the design of the chiller for application on passengers' vessels. Results showed that operation under constant inclination of 30° resulted in a reduction of the cooling energy supplied by 22.5 % for the module with zeolite and by 55.8 % for the module with silica gel. The highest specific cooling energy (SCE) is 0.26 kWh/kg for the zeolite module and 0.18 kWh/kg for the silica gel module. The main issues underlined under tilted operation is the progressive reduction of the water level in the evaporator, which causes incorrect operation of capillary-driven evaporation. Accordingly, the increase of water level in the evaporator was suggested as mitigation strategy. It was however found out that the issue is only relevant if prolonged operation in a tilted condition is foreseen, but not under typical rolling operation with continuous movement.

1. Introduction

International shipping contributed for approximately 2 % of overall world energy-related CO_2 emissions in 2021 [1]. In order to meet the requirements of the Net Zero Emissions by 2050 Scenario, which entails a nearly 15 % reduction in emissions from 2021 to 2030, strong efforts are needed. This includes the use of low- and zero-carbon fuels and technologies for oceangoing vessels, technological innovation, supportive policies, and collaboration across the value chain. Among the different measures needed to reach the decarbonization targets, waste heat recovery has been considered of the essentials. Indeed, in [2], different measures for the reduction of emissions in container ships are evaluated, namely Waste Heat Recovery Systems, Drag Reduction Coatings and Slow Steaming, considering the environmental and economic constraints. It was found out that the most effective combination is speed reduction combined with waste heat recovery. The economics of waste heat recovery in the maritime section is also discussed in [3], where the need for proper data on the actual savings in order to calculate the profitability of the installed solutions is highlighted. Several ways have been proposed over the years for the utilization of waste heat from combustion engines in the maritime application, as discussed recently in [4]. Considering a classification based on the type of demand covered, there are systems for heating demand (waste heat recuperators, boilers, regenerators), systems for desalination applications (mostly multi-effect distillation), technologies for power production, especially ORC, Kalina cycles and turbochargers generators [4]. All of them are making use of the medium-to-high-temperature heat. The only systems that can make use of medium-to-low temperature heat, such as the heat recovered from the jacket coolant of the combustion engine, are sorption systems for cooling and desalination applications [5–7]. The naval sector faces numerous challenges in maintaining optimal working conditions, including the provision of effective cooling systems. Cooling is vital for ensuring crew comfort, preserving the integrity of sensitive equipment, and optimizing overall operational performance [8].

Adsorption cooling has gathered significant interest and

* Corresponding author.
E-mail address: valeria.palomba@cnr.it (V. Palomba).

https://doi.org/10.1016/j.applthermaleng.2024.123224
Received 6 February 2024; Received in revised form 2 April 2024; Accepted 19 April 2024
Available online 21 April 2024

Nomenclature

A	equilibrium potential, kJ/kg
cp	specific heat capacity, kJ/(kg K)
D	is the diffusion coefficient, m/s^2
d_{cryst}	crystallite layer thickness, m
E	constant for the Dubinin-Ashtakov fitting, kJ/kg
f_{geom}	geometric factor, −
h	specific enthalpy, kJ/kg
k	coefficient for the linear driving force model
M	mass, kg
$\dot{m}$	mass flow rate, kg/s
n	constant for the Dubinin-Ashtakov fitting −
$\dot{Q}$	Thermal power, kW
S	surface, m^2
T	temperature, °C
t	time, s
U	internal energy, kJ
u	specific internal energy, kJ/kg
X	uptake, g/g
α	coefficient of heat transfer, $W/(m^2)$

Subscripts

ad	adsorption
de	desorption
eq	equilibrium
ev	evaporator
in	inlet
l	liquid
out	outlet
sorb	sorbent
v	vapour
w	water

Abbreviations

AdHEX	Adsorption Heat Exchanger
D-A	Dubinin-Ashtakov
EC-HEX	Evaporator/Condenser Heat Exchanger
HEX	Heat Exchanger
HT	High Temperature, °C
HTF	Heat Transfer Fluid
LDF	Linear Driving Force
LT	Low Temperature, °C
MT	Medium Temperature, °C
SCE	Specific Cooling Energy, kWh/kg

investigation for maritime applications due to several key advantages it offers over traditional cooling technologies, especially in the harsh conditions of marine environment. These include mechanical stability, due to the lack of moving components, environmental friendliness since adsorption cooling systems do not employ traditional refrigerants, such as hydrofluorocarbons (HFCs), which have high global warming potential. Instead, they utilize adsorbent materials like activated carbon or silica gel, which have negligible environmental impact [9]. This aspect aligns with the growing emphasis on sustainability and reducing greenhouse gas emissions in the maritime sector. Moreover, adsorption cooling systems have the potential to offer higher energy efficiency compared to vapor compression systems under certain conditions, especially in the marine environment [10,11]. The absence of mechanical compression allows for reduced electrical energy consumption and, as state before the use of waste heat or low-grade heat sources, thus reducing fuel consumption.

The evaluation of sorption systems for maritime environment is not new and several papers have discussed it over the last three decades. An overview of the main studies carried out in the last 10 years is reported in [12]. In particular, the oldest studies were mostly concentrating on the production of ice, mostly considering fishing vessels applications [13]. In [6], the case of fishing vessels is still considered, but through cooling generation below zero using a sorption chiller with activated carbon/ethanol working pair. The same chiller was experimentally evaluated in [14]. Another possibility, that showed potential benefits in maritime applications, is the use of sorption chillers as a mean to waste heat recovery for space cooling purposes in passengers' vessels. For instance, the energy and exergy analysis reported in [15,16] show that there is a potential for energy efficiency improvement of the ship (up to 3 %) if waste heat-driven cooling is applied in Nordic climates. The impact of the air conditioning system would be higher in warmer climates, as it is the case of ferries in Southern Europe. Several other studies are available regarding the overall energy efficiency of a sorption cooling system integrated into the overall system of the ship. A complete system for meeting the heating, cooling, and refrigeration needs of a container ship, for example, is modelled in TRNSYS in [19,24], taking into account both the dynamic behavior under realistic conditions and the actual connections of all the system's components. The sorption system's impact on weight and additional fuel consumption was assessed in [6], demonstrating that the advantages of using such a system are solely dependent on the routes used and the length of the cruise. Despite these efforts to prove the feasibility of sorption systems on board, a proper assessment of all the design steps and specific conditions is still lacking. In [17]the waste heat recovery system needed for driving a double-effect absorption system on board Is considered. The application in an aggressive environment, and therefore the corrosion issues, are considered in the design of prototypes as described in [7,18]. However, one missing aspect in design of sorption systems for ships is their actual performance and behavior under the unique and dynamic conditions of a moving ship. The tilting and rolling motions experienced by naval vessels can significantly impact the adsorption process, heat transfer mechanisms, and overall system performance. Indeed, liquid absorption systems have already been tested in such dynamic conditions and the results of tests highlighted the existence of possible critical issues. For instance, the realization of a testing rig for absorption columns using NaOH/air absorption system for CO2 absorption and the tests under different operating conditions are reported in [19]. In this work, tests are carried out in vertical position, under permanent tilting and under rolling conditions. The results are reported in terms of a performance reduction factor and CO_2 limiting diffusion factor. Results highlighted a reduction of performance of about 8 % for 6° permanent tilting, whereas continuous motion did not affect significantly the operation of the column. This is the only reported case in the literature where similar tests are carried out, and it refers to a different case than a chiller that needs to provide continuous cooling effect. Therefore, it is essential to conduct experiments under representative moving conditions to accurately assess the feasibility, performance, and limitations of adsorption chillers in the naval sector.

While the evaluation of sorption systems for maritime environments has been a topic of interest for several decades, our research addresses a critical gap in the existing literature. Specifically, we focus on the operation of sorption modules under swinging conditions, which are inherent during sailing. No prior studies have systematically analyzed sorption systems in this context. Our investigation involves conducting first-of-a-kind tests on sorption modules while the vessel is in motion, considering variable inclinations. By doing so, we aim to shed light on the performance and behavior of these systems under real-world maritime conditions. Furthermore, we employ a validated model in Modelica

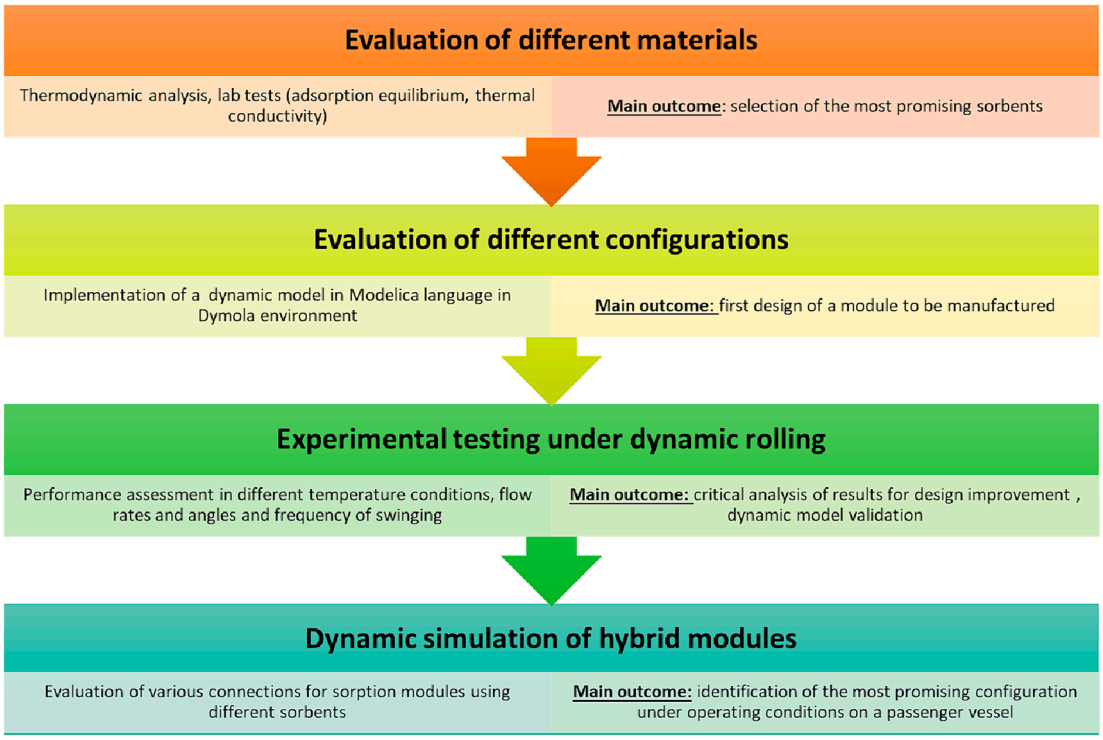

Fig. 1. The methodology used in the present study.

language to design an adsorption chiller optimized for maximum efficiency in maritime applications. This paves the way for improved comfort for passengers and crew: reliable cooling systems enhance the comfort of passengers and crew members during voyages. Efficient sorption chillers can maintain pleasant indoor temperatures even when the ship is in motion. Moreover, energy-efficient cooling reduces fuel consumption and greenhouse gas emissions. By integrating sorption systems, ships can contribute to more sustainable maritime operations.

2. Methodology

The methodology followed considers the limited practical experience on the design and installation of adsorption chillers on board. Indeed, must be taken into account that the operating conditions of the adsorption chillers in maritime environment are quite different from standard conditions for which the commercial units are generally optimised. On the other hand, the possible variability of ambient conditions and of the load have a significant effect on the performance and operating features of the sorption unit. The experience in the testing of such kind of chillers is only limited to stationary applications and therefore there is a significant lack of data for the proper design and sizing for the targeted applications. Accordingly, the experimental results were coupled with dynamic modelling of the system that was used for a critical analysis of the results and a design review of the system.

The activity carried out is schematically presented in Fig. 1: a preliminary design of the adsorption system for application on board was carried out by means of experimental data on commonly employed sorbents and by means of a validated model in Modelica language within Dymola environment, which is described in [20] and more in detail in section 7. Subsequently, the manufactured modules were experimentally investigated, using for the first time in the reported literature, a moving platform to reproduce the operating conditions on board of a passenger ship during the route. Starting from the performance assessment under the investigated conditions, the validated model in Dymola was calibrated and used for the evaluation of possible hybrid configurations on board, i.e. by analyzing the possibility of manufacturing

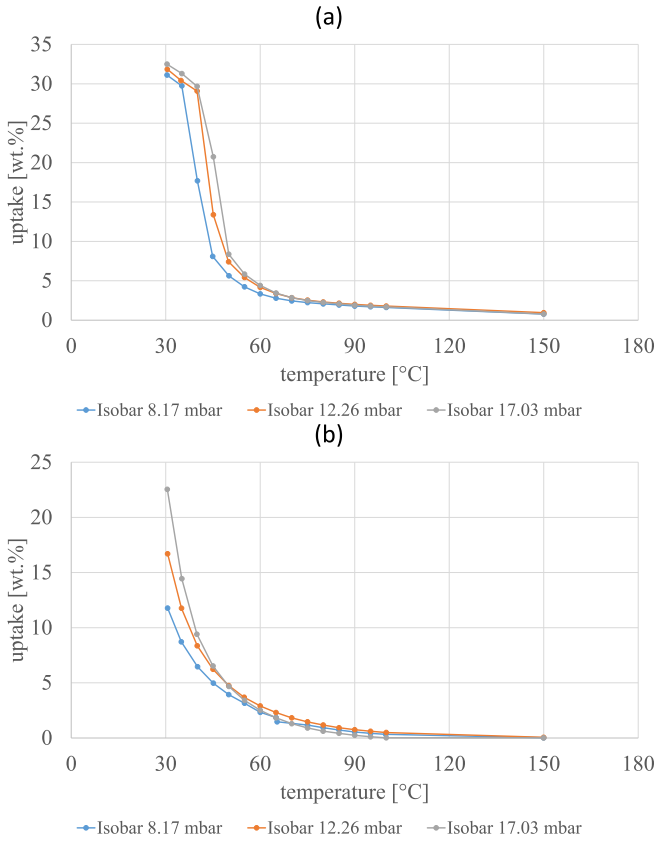

Fig. 2. Adsorption water vapour equilibrium measured over the selected materials. (a) SAPO-34 zeotype, (b) Siogel®.

chillers with modules employing different sorbents.

The experimental tests on the different sorbents and the preliminary design are not in the scope of the present paper, the data on adsorption equilibrium and specific heat of the sorbents selected are given in the supplementary materials.

3. Materials

The adsorbents used for the design of the adsorption chiller in the present studies are silica gel and a zeotype belonging to SAPO-34 class. The silica gel used is supplied by Oker Chemie under the commercial name of Siogel®, whereas the SAPO-34 is directly grown on the surface of aluminum heat exchangers at Fahrenheit GmbH using a patented process. For the evaluation of the maximum adsorption capacity, as well as proper implementation of the model of the modules, the adsorption capacity was measured at CNR ITAE, using an existing thermogravimetric apparatus available. It is a Dynamic Vapor Sorption setup, whose detailed description of the operation is reported in [21].

The equilibrium curves measured are shown in Fig. 2,where isobaric adsorption at different evaporation pressures is shown. It is worth noticing that, as reported in [21], the SAPO-34 shows a slight hysteresis between adsorption and desorption. However, in the operating conditions evaluated in this paper, this causes no influence on the behavior of the system, since proper cycling in repeatable conditions is obtained, as shown in the tests of similar modules with SAPO-34 materials from Fahrenheit which are reported in [22]. In the implementation of the model, the hysteresis was taken into account by using two different equations for the equilibrium curves. The formulation of the equations is shown in the supplementary materials to the paper.

4. Modules design and description

The overall layout selected is characterized by the solution with "process module", which is typically employed by the sorption chiller manufactured by Fahrenheit GmbH, as described for instance in [10,22]. In this layout, the process module consists of two heat exchangers, facing each other. One is the adsorption heat exchanger coated with the sorbent (AdHEX) and one is the evaporator/condenser heat exchanger (EC-HEX). Furthermore, a process module contains a precisely defined quantity of process water (refrigerant), which is retrieved from the adsorption capability of the employed sorbent material under the expected operating conditions. During the adsorption phase, the refrigerant vapour is adsorbed by the sorbent material, hence the pressure in the module decreases and the liquid refrigerant starts evaporating from the surface of the evaporator. In this phase, the cooling capacity is delivered to the user. When the sorbent is completely saturated with the refrigerant, it must be regenerated in the desorption phase. The sorbent is heated up and expels the refrigerant, which condenses onto the condenser. Because the cooling effect is created only during the adsorption phase, to allow quasi-continuous cooling, at least two identical process modules are needed working out of phase.

The main design constraint for the operating conditions on the vessel is to limit/avoid the movements of refrigerant (water) inside the process modules. Limitations and possible issues include refrigerant overflow, refrigerant mixing, and performance losses that are caused by the uncontrolled and unwanted movements of the sorbent and the refrigerant inside the module. Since the sorbent in the adsorption chillers is solid and fixed in the adsorber, the main issue to be solved is how to keep the refrigerant in place and avoid it entering such spots in the process modules in which the refrigerant is not in contact with the evaporator. This phenomenon is often referred to as "false condensation" and occurs when during the desorption phase, the refrigerant vapour condenses on the module walls instead on the EC-HEX surface. Subsequently, during the adsorption phase, this part of the condensate evaporates, but since it has no contact with EC-HEX it is not contributing to the cooling capacity.

These considerations led to two main innovations compared to the standard design:

- The use of heat exchangers in horizontal positions, as shown in Fig. 2. Such layout is expected to eliminate the "false condensation" completely, since the condensate flows always to the bottom of the process module, where the EC-HEX (able to work as flooded evaporator) is located.
- The selection of a new type of EC-HEX, which is a finned pipe heat exchanger. As already demonstrated from previous works in the literature, [23–25] the main advantage of the finned pipe-HEX compared to other configurations, such as the pool boiling, is the lower sensitivity to the position and the use of capillary-assisted operation, which allows achieving high heat transfer rates without the need for a high level of refrigerant and actually work better for small amount of refrigerants (level height almost close to 0). This allows reducing the amount of refrigerant inside the module to the exact quantity needed strictly for processing purposes and avoids refrigerant overflow and mixing.

Two different modules were tested, which mostly differ for the type of sorbent used:

- A module using the zeolite synthesized on the surface of the Ad-HEX according to the patented process by Fahrenheit and described in [26]. The heat transfer area of the EC-HEX is 6 m^2, the amount of sorbent is 4 kg and the process water contained is 2 dm^3.
- A module with microporous silica gel glued on the Ad-HEX. The heat transfer area of the EC-HEX is 11 m^2, the amount of sorbent is 13 kg and the process water contained is 3.7 dm^3.

In order to compare the results, the achievable energies/powers were normalized per mass of sorbent or surface area of the EC-HEX.

5. Experimental

5.1. Testing facilities

The testing rig used for the testing of the modules is described in details in [10,22,27] and the schematics and list of sensors installed are reported in Appendix A. It consists of three water storages for supplying the High Temperature (HT, driving temperature), Medium Temperature (MT, condensation/adsorption temperature) and Low Temperature (LT, evaporation temperature) for the operation of the adsorption modules tested. The HT storage is a 1.5 m^3 storage connected to a gas boiler and an electric heater, the MT storage is a 1 m^3 storage connected to an air-to-water chiller and can be heated up by means of an immersed electric heater, the LT storage is a 0.75 m^3 storage including 30 % water/glycol mixture connected to another air-to-water chiller and includes immersed electrical resistances for increasing the temperature. The temperature regulation on the three circuits of the system under testing is achieved by means of high-speed valves from Siemens mixing between inlet and outlet from the storage tank. Hydraulic separation between the testing rig and the system under testing is achieved by using plate heat exchangers.

An Edmolift ART 750 lifting platform with hydraulic actuators was used to move the modules under test. It has one vertical translational and one rotational degree of freedom, has a maximum capacity of 750 kg and makes a 45° rotation in 30 s.

The P&ID of the testing rig is shown in Fig. 4. As it is possible to notice, the testing rig mainly consists of tanks that are connected to heat sinks or sources. Their temperature is set within a few degrees of the desired one for the specific circuit (HT, MT, LT). The three circuits from the testing rig are separated from the ones of the chiller under testing by means of plate heat exchangers. Each circuit is equipped with a variable speed pump and with an expansion vessel and safety valves.

Since the modules to be tested are not equipped with valves for

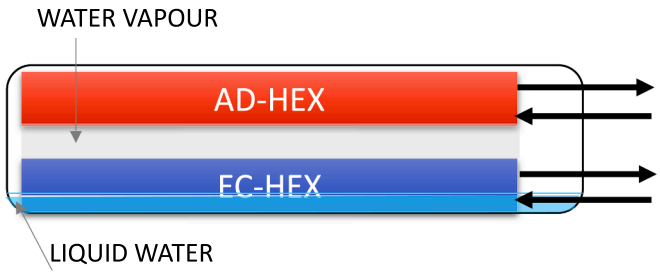

Fig. 3. Layout of the process modules for the experimental testing.

switching between desorption-condensation and adsorption-evaporation phases, a hydraulic group was realised which, by means of solenoid valves, manages the connections between the module and the testing rig. The hydraulic group is shown in Fig. 3 (left), whereas the modules on the lifting platform and connected to the testing rig are shown in Fig. 3 (right).

5.2. Testing procedure

The experimental test session begins with the conditioning of the thermal storage systems. After the storage systems of each of the three circuits have reached the predefined temperatures, the test is started.

When the test is started, since a single module per time is being tested, the valves on the hydraulic group which connected the adsorber to the HT circuit and the evaporator/condenser to the MT circuit are open. During the first half cycle, desorption occurs and the evaporator/condenser operates as a condenser for the refrigerant. During the second half cycle, the adsorber is connected to the MT circuit and the evaporator/condenser (which operates as an evaporator for the refrigerant) is connected to the LT circuit. This is achieved by automatically changing the position of the solenoid valves. The process module takes approximately 5 cycles to reach a steady state operating condition.

Three types of tests were realized:

- Fixed process module in horizontal position (indicated as "0° static" in the following). This test represents the reference data for benchmarking.
- Fixed inclined test (indicated as "30° static" in the following). During the test, the desired degree for the platform is set and maintained throughout the test.
- Moving test (indicated as "tilting" in the following). During this test, a rotation of a predefined amplitude is performed in alternating directions every 30 s.

The selection of the amplitude of the angles of inclination was selected in accordance with the specifications for testing hydraulic, electrical, electromechanical and electronic systems prescribed in the "DNVGL-CG-0339" standard, which prescribes that systems and equipment intended for gas tankers and chemical tankers remain functional up to an inclination angle of 30° [28]. The standard does not prescribe a specific frequency of variation according to waves. However, it was decided to test also a case with variable inclination. To this aim, the frequency of the rotations imposed by the platform and their speed were selected on the basis of preliminary analyses carried out on ships in service in the Mediterranean Sea regarding the accelerations produced by the wave motion on passenger vessels. The detailed modelling of these conditions is out of scope of this paper, but the methodology followed is described shortly. The ship motion can be schematically considered as the motion of a large mass (the ship) on top of a spring. Imbalances on this model (waves) make the ship move. Ship motions, velocities and accelerations are expressed in terms of response amplitude operators and are typically expressed per meter wave height. Ansys AQWA software was used for identifying the motions in x,y and z directions according to the guidelines from DNVGLCG-0130 standard. It was found out that the maximum velocity expected is 0.4 m/s. As it will be shown in the results section, a slow and low frequency movement represents a more unfavorable condition than a fast and high frequency movement. Therefore, by adopting a period of 30 s for the moving test, conservative conditions are considered.

5.2.1. Testing conditions and data analysis

The main aim of the tests was to compare the performance of the modules between the static "traditional" operation and the typical operation under static or moving inclination cases. Moreover, one of the peculiarities of the installation on board of vessels is that the operating temperatures are usually stable, since they are regulated by means of mixing/deviating tempering valves at a fixed value. Therefore, the comparison was carried out considering two operating cases, corresponding to mild and warm seawater temperatures.

- 85 °C (HT), 27 °C (MT), 16 °C (LT).
- 85 °C (HT), 35 °C (MT), 16 °C (LT).

More in detail, the HT temperature corresponds to the inlet temperature temperature of the heat transfer fluid entering the adsorption module, at which regeneration of the sorbent occurs. It is the temperature that can be obtained out of the coolant of the engine on the ship. Generally, this is set at 90 °C, but 85 °C was considered, taking into account the need for a separation HEX with a ΔT of 5 K. The LT temperature is the temperature at which cold is supplied to the user, it depends from the cold distribution system. The value of 16 °C was selected in the present study according to the information obtained by owners of ferry companies. Finally, the MT temperature corresponds to the inlet temperature entering the condenser and the adsorber during the heat rejection phase to the ambient. The heat transfer fluid flow rates used for tests are the nominal ones prescribed by the manufacturer of the

Table 1
List of tests.

SAPO-34	HT	MT	LT	angle	LT flow rate	Silica gel	HT	MT	LT	angle	LT flow rate
	85 °C	27 °C	16 °C	0° static	3000 l/h		85 °C	27 °C	16 °C	0° static	6000 l/h
	85 °C	27 °C	16 °C	0° static	6000 l/h		85 °C	27 °C	16 °C	10° static	6000 l/h
	85 °C	27 °C	16 °C	30° static	6000 l/h		85 °C	27 °C	16 °C	30° static	6000 l/h
	85 °C	27 °C	16 °C	30° tilting	3000 l/h		85 °C	27 °C	16 °C	30° static half cycle	6000 l/h
	85 °C	27 °C	16 °C	30° tilting	6000 l/h		85 °C	27 °C	16 °C	30° tilting	6000 l/h
	85 °C	27 °C	16 °C	20°static	6000 l/h		85 °C	27 °C	16 °C	20°static	6000 l/h
	85 °C	27 °C	16 °C	20° tilting	6000 l/h		85 °C	27 °C	16 °C	20° tilting	6000 l/h
	85 °C	35 °C	16 °C	0° static	3000 l/h		85 °C	35 °C	16 °C	0° static	6000 l/h
	85 °C	35 °C	16 °C	0° static	6000 l/h		85 °C	35 °C	16 °C	10° static	6000 l/h
	85 °C	35 °C	16 °C	30° static	6000 l/h		85 °C	35 °C	16 °C	30° static	6000 l/h
	85 °C	35 °C	16 °C	30° tilting	3000 l/h		85 °C	35 °C	16 °C	30° static half cycle	6000 l/h
	85 °C	35 °C	16 °C	30° tilting	6000 l/h		85 °C	35 °C	16 °C	30° tilting	6000 l/h
	85 °C	35 °C	16 °C	20°static	6000 l/h		85 °C	35 °C	16 °C	20°static	6000 l/h
	85 °C	35 °C	16 °C	20° tilting	6000 l/h		85 °C	35 °C	16 °C	20° tilting	6000 l/h

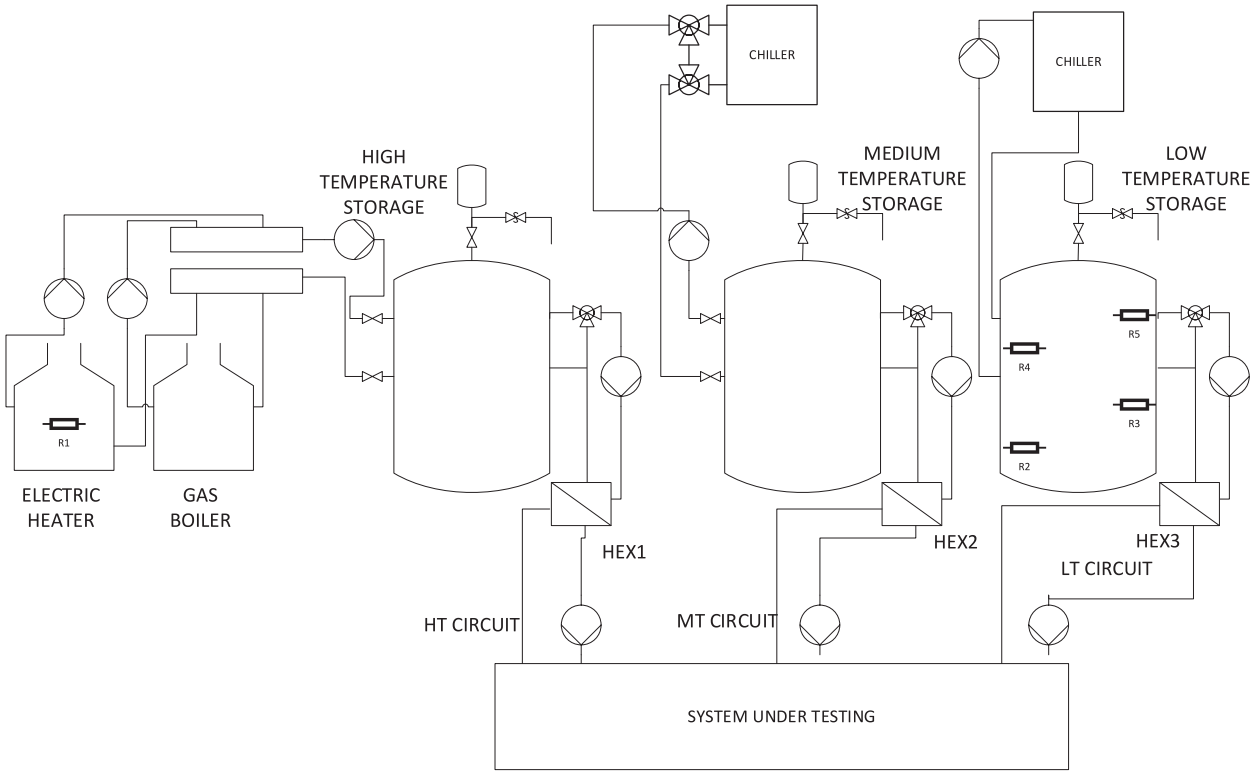

Fig. 4. P&ID of the testing rig.

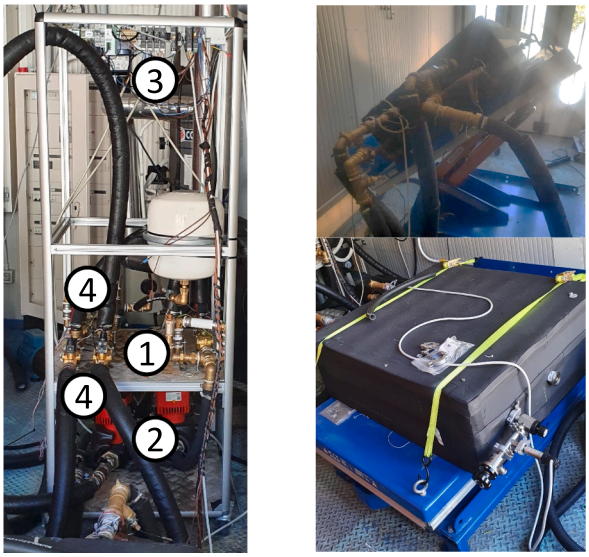

Fig. 5. Left – hydraulic group for managing the sorption cycle; right – the modules under testing 1. Hydraulic valves for switching between the different circuits during the cyclic operation of the chiller; 2: pump; 3: data acquisition system; 4: connecting pipes to the module.

modules: 1.2 kg/s for the LT circuit, 1.6 kg/s for the HT and MT circuits. Preliminary tests were carried out to identify the cycle time to be used. In order to have a fair comparison among the two modules, whose sorbents have different dynamics, the choice of a cycle time that allows the completion of the adsorption for both cases was made, corresponding to a phase time of 500 s. This is also related to the choice of comparing the modules only in term of achievable power and overall energy produced over a typical cycle time. This choice penalizes the COP of the module with the faster dynamics, but, as already discussed by some of the authors in [11], the amount of heat available in maritime applications for waste-heat-to-cold purposes is much higher (even one order of magnitude higher) than the one needed for the targeted applications. Therefore, the COP does not represent a key parameter for the application.

The thermal power of each hydraulic circuit was calculated as:

$$\dot{Q} = \dot{m}\, c_p\, (T_{in} - T_{out}) \tag{1}$$

In addition, the overall energy at the evaporator, which represents the useful effect for the application, was calculated as:

$$Q_{ev} = \int \dot{m}\, c_p\, (T_{in} - T_{out})\, dt \tag{2}$$

The overall list of tests carried out is given in Table 1.

6. Results

6.1. SAPO34 module

The most interesting results during the tests carried out are shown in Fig. 4 and Fig. 5, where a comparison among different operating cases is presented. The typical trends of temperatures are presented in the Supplementary Materials. In particular, Fig. 4 shows the dynamic trend of the evaporation power for a test under 85-27-16 conditions for three operating modes using nominal flow. For simplicity sake, three cycles are shown. Cycle time is 1000 s, but, since only a single module is tested, the useful effect covers 500 s only. The maximum power measured, during the first seconds of the cycle, is 30 kW. It is worth mentioning that this high power is due to the peculiar operation of Fahrenheit's modules: since there is a single HEX working as both evaporator and condenser, during the first seconds of the cycle, when the cycle phase is changed, and the HEX is connected to the LT circuit of the testing rig, there is a sudden drop from the condensation temperature to the evaporation temperature. However, this value, which is measured for just a few seconds, is not representative of the real operating capacity of the

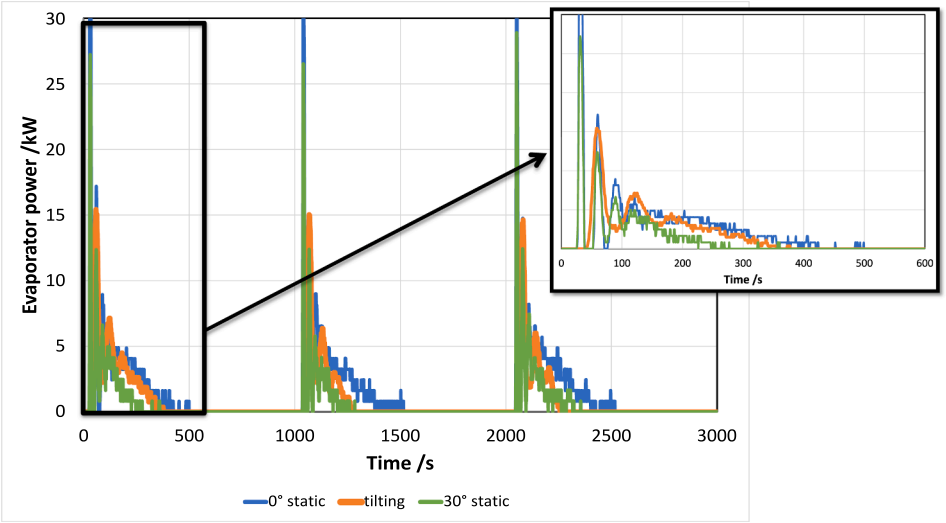

Fig. 6. Example of dynamic trends for cooling power (measured at the HTF circuit of the evaporator) for the SAPO34 module (85-35-16 test). A zoom on the first 500 s is reported on the right.

module. This is the reason for a zoom on the first seconds using a smaller scale on the y axis. The same considerations can be applied to the case of the silica gel module tests in the next section.

It is possible to notice that for the horizontal case (0° static in the picture, blue line), the useful effect lasts longer. The 30° tilting and 30° static cases have a similar behavior, but for the tilting case (orange line in the picture) the average evaporation power is slightly higher. A comparative analysis, in terms of cooling energy in the HTF circuit of the evaporator, is presented instead in Fig. 5. Several operating modes are evaluated using this parameter: beside the previous cases (0° static nominal flow, 30° static and 30° tilting), also the possibility of reducing the flow rate at the evaporator (0° static reduced flow) and having a lower inclination (20° static) are taken into account. The reason for the tests with reduced flow at the evaporator will be better clarified in section 7.2: when considering hybrid chillers configuration, if the circuits from different modules are connected in parallel, the need for high pumping power emerges, and therefore the possibility of reducing the power consumption of the pumps was experimentally explored. The results in Fig. 5 correspond to the dynamic trends from the previous picture, and therefore there is a progressive increase in the energy at the evaporator during the 500 s in which the chiller supplies a useful effect and a plateau during the regeneration phase. It is possible to notice that the energy supplied clearly reduces passing from the 0° case to the inclination ones, i.e. for the specific case of this test is 3 times higher than the tests at 20° and 30° static inclination (purple and green lines in the picture). The 30° tilting case, in which the inclination is periodically changed, shows a better performance, even though lower than the horizonal position. The reasons for the behavior will be discussed more in detail in section 6. It is also possible to notice that the reduced flow is not effective as well, since it penalizes the heat transfer in the heat exchanger and therefore, for the subsequent analyses, only the nominal flow rates will be used.

An overall comparison of all the operating modes analysed is reported in the chart from Fig. 6, where the average energy measured in the HTF circuit of the evaporator in multiple tests with 4 cycles duration is shown. The data considered are for the testing conditions (85-27-16). The results are in line with what reported in Fig. 5: there is always a penalization when comparing the position under inclination with horizontal position (i.e. standard operation). The penalization is higher for the 30° and 20° static tests if compared to the 30° tilting and 20° tilting tests, even though the difference between the static and tilting test at each inclination is only in the order to 10 %. Compared to the results in Fig. 6, the difference between the horizonal tests and the ones with

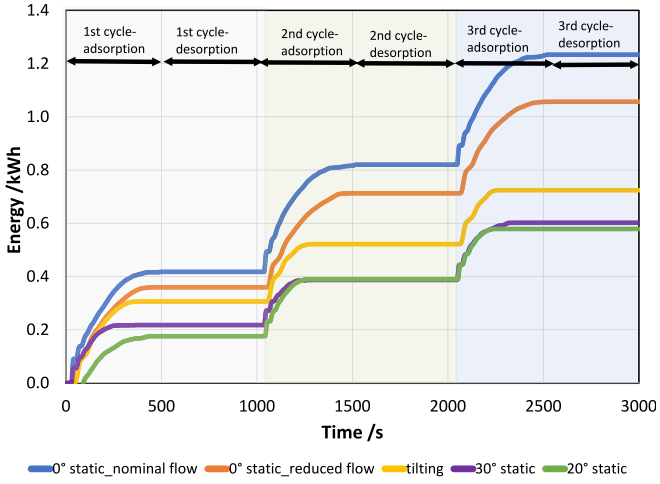

Fig. 7. Energy trends for evaporator for the SAPO34 module at different inclinations (85-35-16 test).

inclination (either tilting or static) is lower and within 35 % and 45 %. Interestingly, the tilting test with reduced flow showed a better performance (higher energy) than the nominal flow, which might actually be due to the possibility of reading a useful temperature difference (i.e. >1 K) for a longer time. It is worth mentioning that all the results are normalized according to the mass of sorbent, in order to allow for better design considerations for the subsequent analyses reported in section 6.

6.2. Silica gel module

The most interesting dynamic trends exemplary results for the silica gel module are presented most in Fig. 7 and Fig. 8. In particular, Fig. 7 shows the dynamic trend of the evaporation power for a test under 85–35-16 conditions for three operating modes using nominal flow. For simplicity sake, two cycles are shown. It is possible to notice that for the horizontal case (0° static in the picture, orange line), the useful effect lasts longer and there is actually still quite high power (up to 5 kW) at the end of the 500 s. The different 30° static tests reported are three: 30° static (the condition described in 4.3), 30° static only condensation – i.e. a test in which the 30° inclination was kept fixed only during condensation and then the rest of the test is at 0° i.e. horizontal condition – and

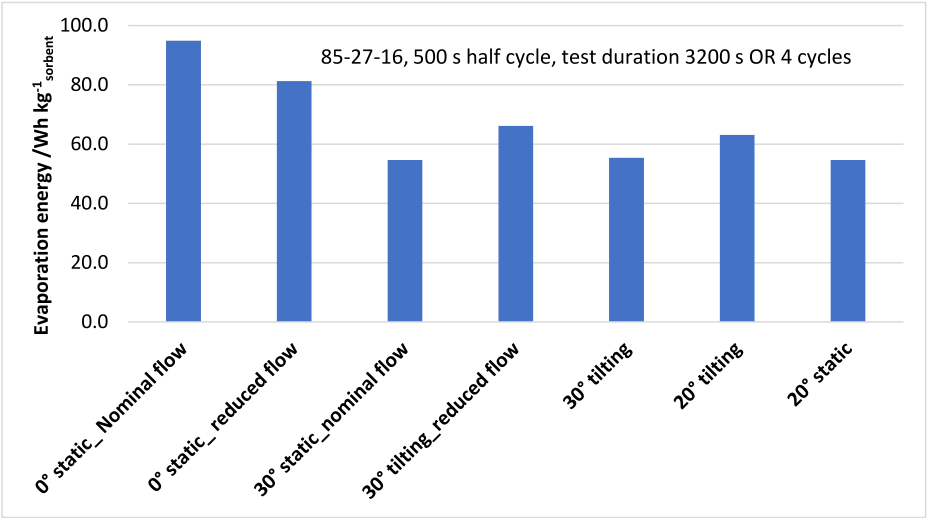

Fig. 8. Evaporation energy for a test under 85-27-16 temperature conditions for a fixed duration of 4 cycles under different operational modes.

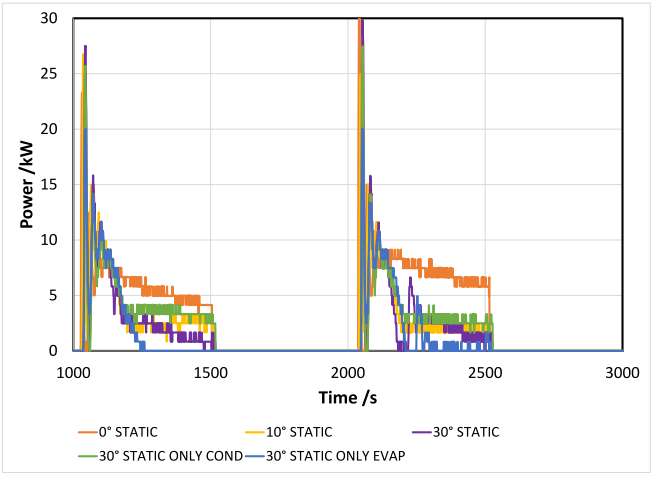

Fig. 9. Example of dynamic trends for cooling power (measured at the HTF circuit of the evaporator) for the silica gel module (85-35-16 test).

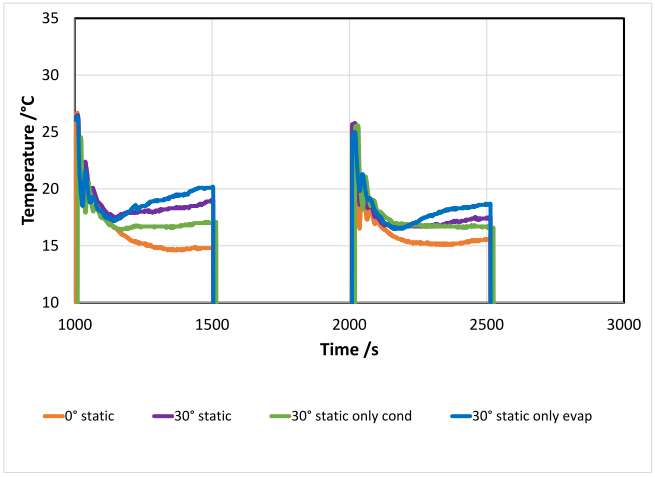

Fig. 10. Dynamic trends for outlet temperature at the evaporator HTF circuit for different operating modes (85-35-16 test).

30° static only evaporator. The latter refers to a test in which the 30° inclination was kept fixed only during evaporation phase and then the rest of the test is at 0° i.e. horizontal condition. It is possible to notice that the "30°static" and "30° static only evaporation" are the most penalized scenarios, whereas keeping the system tilted during condensation only is affecting less the evaporation phase.

Fig. 8 shows which is the actual effect of the tilting / inclined operation on the HTF circuit that represents the user, by comparing the dynamic trends of temperatures outlet (inlet temperature is comparable for all tests). For the 0° static horizontal operation, the temperature is gradually decreasing during the first part of the test and then keeps stable at 15 °C. A similar trend is observed for the "30° static only condensation" case but with a higher temperature for the plateau (16.5 °C). On the other hand, for the other tests, the temperature has a steep reduction at the beginning of the test, but the stabilization occurs only for less than 100 s and then the temperature rises again because the module is not able to keep the same cooling power (no control on the flow rate is made to keep a constant ΔT).

An overall comparison of all the operating modes analysed is reported in the chart from Fig. 9, where the average energy measured in the HTF circuit of the evaporator in multiple tests with 4 cycles duration is shown. The testing conditions considered are for the case 85-27-16. The results are in line with what reported in Fig. 6: there is a penalization when comparing the operation under horizontal position with the inclined ones. As already shown for the SAPO34 module, the penalization is higher for the 30° and 20° static tests if compared to the 30° tilting and 20° tilting tests. In this case, the difference between the horizonal tests and the ones with inclination (either tilting or static) is lower than for the case of the zeolite module, with a difference between the static and tilting test at each inclination in the order of 20 %. The lower difference between horizontal and tilting tests compared to the SAPO34 module can be explained by the fact that the module with silica gel in loose grains has a slower dynamics compared to the one with the synthetized SAPO34 and therefore the effect of the progressive level reduction of water in the evaporator, which will be discussed more in detail in section 7, is less evident.

For the sake of comparison, the conditions that were tested for both modules are reported in Fig. 11.

7. Discussion

7.1. Evaporation performance under different inclinations

The outcome of the results from the tests presented previously is that

there is an actual effect of the operation under inclined or moving conditions, which had never been evaluated before for adsorption chillers. The main reason for the worse operation for the tested layout can be explained according to the schematics from Fig. 10: when the system is in horizontal position the amount of water actually in contact with the pipes of the evaporator HEX is much higher than during 30° operation. Since the evaporator HEX is exploiting capillarity for operation, the smaller wetted area deteriorates its performance, as discussed for instance in [23,25,29]. A possible solution could be represented by the increase of the amount of water inside the evaporator. However, there are two effects which have to be taken into account: for the specific configuration with a single HEX working as evaporator/condenser, increasing the amount of water also means increasing the cooling capacity spent for cooling down the liquid inside the HEX at each half cycle (corresponding to the switch from evaporator to condenser operation or vice versa). At the same time, increasing the amount of water inside the evaporator, can induce submersion of a part of the HEX at the beginning of the evaporation process, thus lowering the performance of the HEX. The mechanism described above also explains why the performance, when operating under 20° static or 30° static conditions, is worsening throughout the evaporation process duration: the amount of water inside the evaporator decreases continuously during the process and therefore the wetted area becomes smaller with time.

The minimum quantity of working fluid used in the prototypes under examination means that the lower exchanger (EC-HEX) is not completely flooded and that the free surface is not at a height sufficient to wet the finned tubes when the modules are in horizontal position. Tilting the unit causes the submersion of a part of the battery of pipes, favoring evaporation by capillarity. This benefit, with the continuation of evaporation, would be nullified by the impossibility of exploiting the exchange surface of the finned tubes emerged due to the inclination, which cannot exchange heat with the liquid phase of the working fluid. At the same time, a fraction of the liquid phase is found in the communication ducts between the two chambers and does not take part in the thermodynamic transformation.

By cyclically repeating the inclination, it is possible to obtain the alternation of these two favorable conditions. The fact that the experimental investigation confirmed that it is the evaporation phase that suffers the most from the effect of the inclination proves this hypothesis.

7.2. Design considerations

Starting from the results presented and the consideration from the previous section, a proper sizing of the modules should be carried out for the specific application, that will represent the starting point for the simulations on the hybrid chiller configuration reported in the next section. The starting point for the analysis was the SCP, Specific Cooling Power, defined as the ratio between the average cooling power and the mass of dry sorbent:

$$SCP = \frac{\dot{Q}_{ev}}{m_{sorb}} \tag{3}$$

Under 0° static operation, the SCP calculated are 1.3 kW/kg for the SAPO34 module and 0.6 kW/kg for the silica gel one. Considering that the configuration tested (one module) does not allow for heat recovery, which would increase the SCP by around 15 % [30], we can estimate that for a 20-kW cooling power module a proper size would require 13.4 kg of zeolite and 29 kg of silica gel. However, considering the reduction of the cooling power due to the inclination, for the dynamic case, which is mostly likely to occur under operation during vessel's route, the average cooling energy reduction was 22.5 %. Accordingly, an estimation of 15.4 kg of zeolite and 35 kg of silica gel could represent a proper initial design point.

In the typical analysis of adsorption chillers, the Coefficient of Performance is generally used for the analysis. In the configuration tested in the present case, with a single module instead of the typical configuration with two modules operating in counterphase, there is no possibility for heat recovery. This strategy is typically applied in the vast majority of the most recent prototypes and commercial systems whose performance maps are available in the literature or online. Due to the impossibility of applying the heat recovery strategy, the COP values measured are not comparable with the current state-of-art and it was therefore decided to omit the value in the calculations. Moreover, considering the large amount of waste heat available on board of vessels, it can be argued that the optimization of the thermal COP will not represent a critical issue. On the contrary, the most relevant parameter for the adsorption chiller installation is the power density, which reflects on the volume occupied on board."

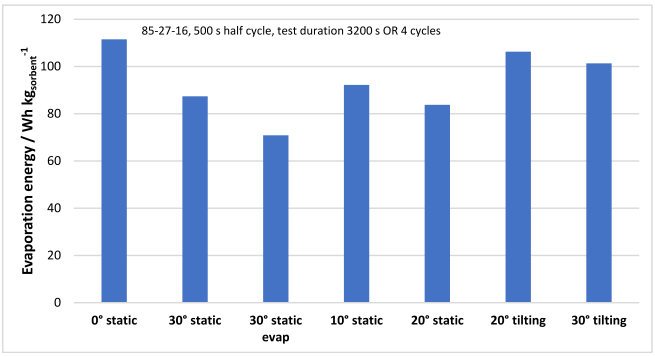

Fig. 11. Evaporation energy for a test under 85-27-16 temperature conditions for a fixed duration of 4 cycles under different operational modes.

The main conclusion that can be drawn according to the results presented so far is that, one the one hand, there is the need to properly define the amount of water inside the heat exchanger to reduce the effect of movement in terms of wetted level. It has been demonstrated in [23,25,29] that the capillary-driven evaporation is much more efficient than other methodologies, so the use of this type of evaporators is still to be preferred. However, it follows that it would be needed to oversize the adsorption chiller. Accordingly, starting from the experimental results obtained, an alternative approach was followed: the use of a "hybrid" layout, i.e. the use of modules with different sorbent materials inside the same adsorption chiller. The underlying idea is that, by exploiting more efficiently the peculiarities of the two different sorbents (silica gel and SAPO-34), it is possible, with the same heat source temperature and power, either increase the cooling or reduce the outlet temperature. To this aim, this alternative strategy is evaluated in section 8.

8. Hybrid chiller configuration

The results of the experimental activity not only indicate the need for oversizing the chiller if a long-time operation under tilted conditions is foreseen, but can also be further used for the selection of the most adequate configuration for the application. In particular, the case of different configurations for a hybrid chiller, i.e. a chiller combining silica gel and zeolite couples of modules, was studied. Three configurations were evaluated, which are reported in Fig. 14:

– Parallel connections of the three circuits for the two modules, which corresponds to the two modules operating separately (Fig. 11a). In this configuration, a silica gel module and a zeolite module are present. Considering the parallel connection, this means that the two modules are desorbing/condensing and adsorbing/evaporating at the same time. To achieve a continuous effect, two couples of modules would be needed, working in counterphase (e.g. while one silica gel module and a zeolite module are desorbing, the other two are adsorbing and viceversa).

– Parallel connection of HT and MT circuits and serial connection of LT circuit, with the silica gel module as the topping one. In this case the silica gel module acts as a pre-cooling system for the LT circuit of the zeolite module (Fig. 11b). The HT and MT circuits are connected in parallel, which means that during desorption the same case as before (case a) occurs. However, during adsorption/evaporation phase, the return HTF from the LT circuit enters firstly in the silica gel module and is pre-cooled. The pre-cooled HTF enters the zeolite module and then is delivered to the user.
– Parallel connection of MT circuits and serial connection of HT and LT circuits. The zeolite module is the topping module for the HT circuit, since it requires the higher regeneration temperature; the silica gel module is the topping module for the LT circuit (Fig. 11c). In this case, the return HTF circuit from the waste heat recovery circuit enters at first in the zeolite module. It then exits from the zeolite module and enters the silica gel module, the exit from the silica gel module represents the inlet to the waste recovery circuit. The LT circuits are connected as in the previous case: the return HTF from the LT circuit enters firstly in the silica gel module and is pre-cooled. The pre-cooled HTF enters the zeolite module and then is delivered to the user.

As already discussed in the introduction, hybridization of sorption chiller in various applications, including the maritime field, has gained interest in recent times in the literature. Hybrid chillers studied are, in the vast majority of cases, combinations of adsorption chiller and vapour compression chillers. However, in the maritime environment, where the electricity is mostly generated by means of generators attached to the main engine or auxiliary engine, saving of electricity is a key priority for reducing fuel consumption. Accordingly, the use of a fully thermally driven system can be beneficial, provided that temperature control in the operating ranges can be achieved and adequate cooling power is provided. Accordingly, the configurations shown in Fig. 11 were simulated and compared in terms of powers needed / extracted at each circuit and average temperatures/ minimum temperatures in the LT circuit.

8.1. Model implementation

The dynamic model implemented is based on the SorpLib library, which is a library of components modelled using Modelica language and realised by the Institute of Technical Thermodynamics at RWTH Aachen university [31]. Starting from such an approach, a library of calibrated components, based on experimental investigation of sorption dynamics of different configurations, was developed by CNR and is extensively described in [20]. The main equations used in the implemented model are described in the following.

8.1.1. Sorption equilibrium curves

The adsorption equilibrium uptakes of SAPO34 directly crystallized by Fahrenheit and Siogel were implemented according to the measurements carried out at CNR. Both curves can be described by the Dubinin-Astakhov (D-A) equation, as discussed in [21]. Moreover, to better describe the different sorption equilibrium curves of adsorption and desorption phases, namely the hysteresis phenomenon, a logical parameter – status_hysteresis is introduced, and the sorption equilibrium curves are described as follows:

$$X_{eq} = \begin{cases} X_{0,de} exp\left[-\left(\frac{A}{E_{de}}\right)^{n_{de}} \right], \; status\_hysteresis = 1 \\ X_{0,ad} exp\left[-\left(\frac{A}{E_{ad}}\right)^{n_{ad}} \right], \; satus\_hysteresis = 0 \end{cases} \quad (4)$$

The parameters for the D-A equation are presented in the supplementary materials.

8.1.2. Adsorber modelling

The adsorber model includes the equations for heat and mass transfer. Heat balance of the adsorber is given by:

$$\frac{dU_{sorb}}{dt} = u_w \cdot \frac{d(M_w)}{dt} + \left(M_w c_{p,w} + M_{sorb} \cdot c_{p,sorb}\right) \cdot \frac{dT_{sorb}}{dt} = \dot{M}_{w,in} h_{in} - \dot{M}_{w,out} h_{out} + \dot{Q}_{sorb,htf} \quad (5)$$

where U is the internal energy [J], u is the specific internal energy [J/kg], M is the mass [kg], cp is the specific heat [J/(kg K)], T is the temperature [K], h is the specific enthalpy [J/kg] and $\dot{Q}_{sorb,htf}$ [W] is a term indicating the heat transfer between the heat transfer fluid and the sorbent. The subscripts "w" refers to water, whereas "sorb" to the sorbent material.

The heat exchanged with the heat transfer fluid is given by:

$$\dot{Q}_{sorb,htf} = (\alpha S)_{HEX} \cdot \left(T_{htf} - T_{sorb}\right) \quad (6)$$

with $(\alpha S)_{HEX}$ being the overall heat conductance between metal and sorbent. It includes: the thermal contact resistance between flat tube and lamella, the thermal conductivity of the lamella, and the thermal conductivity of the directly crystallized sorbent.

The mass balance equation is:

$$\frac{dM_w}{dt} = \dot{M}_{w,in} - \dot{M}_{w,out} \quad (7)$$

The change in adsorbate mass is usually derived according to the linear driving force (LDF) approach. A more detailed derivation of the LDF approach and its limitations can be found in previous works [32,33] and can be expressed as:

$$\frac{dX}{dt} = \frac{1}{M_{sorb}} \cdot \frac{dM_w}{dt} = k_{LDF} \cdot (X_{eqi}(p,T) - X) \quad (8)$$

where X is the uptake [kg/kg], X_{eqi} refers to the uptake at equilibrium under the current pressure and temperature conditions and k_{LDF} is the diffusion coefficient. For the application of this approach to dense directly crystallized layers of SAPO-34 it is possible to use the proposed form by Velte et al. [34]:

The constant LDF parameter k_{LDF} is calculated as shown in equation 9 depending on the adsorbate diffusion coefficient

$$k_{LDF} = f_{geom} \cdot \frac{D_{sorb}}{d_{cryst}^2} \quad (9)$$

where D_{sorb} [m/s^2] is the diffusion coefficient, d_{cryst} [m] is the characteristic crystallite layer thickness and f_{geom} is a geometric factor depending on the features of the used heat exchanger.

8.1.3. Condenser/evaporator modelling

The evaporator/condenser model developed is based on the implementation already described in [35] and includes the heat and mass transfer equations for the refrigerant which is in vapor/liquid equilibrium conditions. The equations for heat and mass transfer are:

$$\frac{dM}{dt} = \dot{m}_v + \dot{m}_l \quad (10)$$

$$\frac{dU}{dt} = \dot{H}_v + \dot{H}_l + \dot{Q}_{w,htf} \quad (11)$$

where the subscripts "v" and "l" refer to vapour and liquid refrigerant, respectively. The heat exchanged between the refrigerant and the heat transfer fluid is:

$$\dot{Q}_{w,htf} = (\alpha S)_{HEX} \cdot \left(T_{htf} - T_w\right) \quad (12)$$

The model validation is shown in Appendix B.

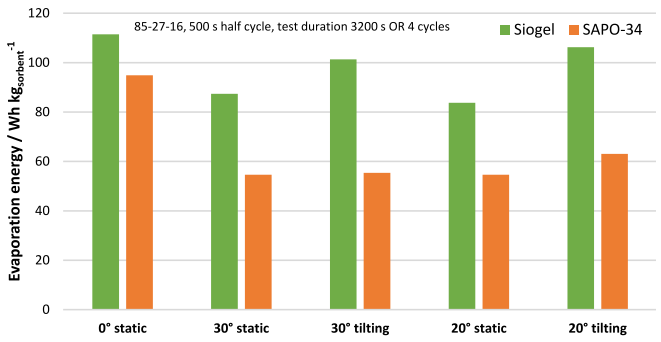

Fig. 12. Evaporation energy for tests under 85-27-16 temperature conditions for a fixed duration of 4 cycles under different operational modes- comparison of the modules.

8.2. Results

As exemplary case, the results for the following operating conditions are reported: HT_{in}: 85 °C, MT_{in}:35 °C, LT_{in}: 14 °C. Such conditions correspond to a severe condition in the MT circuit, whereas HT and LT circuits temperatures are less variable since they are not depending on the specific operating routes but on the regulation of the cooling water loop from the engine and the cold distribution loop, whose temperatures are not varying in a wide range for the different passengers' vessels. The mass of sorbents used in the simulations is 15 kg for the zeolite modules and 35 kg for the silica gel modules (thus considering the need for oversizing the system compared to what tested in the lab), considering an architecture with two module pairs working in counterphase, to have a continuous cooling effect. The flow rates considered are 10 m^3/h for the MT circuit and 5 m^3/h for the LT and HT circuits of each module pair. This means that for parallel connection of a circuit, a double flow rate from the heat source/sink is needed.

In the case of the configuration (a), i.e. all circuits in parallel, the dynamic trends shown in Fig. 12 indicate the main drawback of such a configuration: the cooling effect is discontinuous, in the sense that, since the cooling power achievable by the zeolite module and the silica gel module is different, the outlet temperatures that are achieved are due to the flow mixing of the two streams from the modules, and therefore the overall achievable LT outlet temperature is higher (12.1 °C). At the same time, having all the circuits in parallel requires having higher flow rates and therefore higher pumping power and electricity consumption for it. The average cooling power achievable is 21 kW for the zeolite modules and 16 kW for the silica gel modules, for an overall cooling effect of 18.5 kW in average.

The configuration (b) allows achieving lower outlet temperatures in the LT circuit, due to the fact that there is a pre-cooling effect of the silica gel module, with values as low as 7 °C and 9 °C as average which allows even the efficient use of fan coils as cold distribution system, as shown in Fig. 13. The main drawback of this configuration is that it requires a higher pumping power in the HT and MT circuits, for which parallel operation is foreseen. The average cooling power achievable is 17.1 kW. The lower values compared to the previous case is mostly related to the fact that the zeolite modules work under less favourable conditions (i.e. lower evaporation temperature). This configuration is therefore preferable mostly if there is a need for reducing the chilled water outlet (i.e. to match the operating temperature of the installed cold distribution system).

Configuration (c) shows results, in terms of average cooling power, similar to the previous case, i.e. an average cooling power output of 17 kW. This is due to the possibility of efficiently regenerating the silica gel also at lower temperatures. Indeed, as shown in Fig. 14, the average temperature difference between the modules with different sorbents is in the range of 8 K, which indicates an average regeneration temperature of 81 °C for the silica gel modules. As reported in the literature, such temperatures are sufficient for adequate regeneration of the material and allow, at the same time, to use a lower amount of heat from the coolant circuit of the engine and a lower flow rate and therefore pumping power needed.

Such results indicate that the configuration that would perform better, and allows the maximum flexibility in operation on board of passengers' vessels is the configuration (c), with serial connection of HT and LT circuits of different modules. Compared to the use of a larger chiller with identical module pairs this allows two advantages: the possibility of using, for one of the two module pairs, a cheaper sorbent (silica gel) and the possibility of reducing the overall amount of heat needed thanks to the series connection of the HT circuits. At the same time, with such a configuration, chilled water outlet temperatures compatible with both the operation of fan coils and radiant ceiling/floors can be achieved. In case the desired target is instead the maximization of the power output, the selection of a system with 2 zeolite module pairs or 2 zeolite modules + 2 silica gel modules is suggested.

In order to further compare the three configurations, the outlet temperature at the evaporator HTF circuit are reported in Fig. 15 and Fig. 16, whereas the temperatures for the adsorbers in configuration (c) are shown in Fig. 17 and the cooling power is shown in Fig. 18. As previously discussed, the average cooling power is higher for configuration (a), with a minimum difference for configuration (b) and (c) but the outlet temperature in the configurations (b) and (c) is in average 3 K lower, thus making the adsorption chiller also suitable for operation with fan coil or low temperature cooling distribution system. As

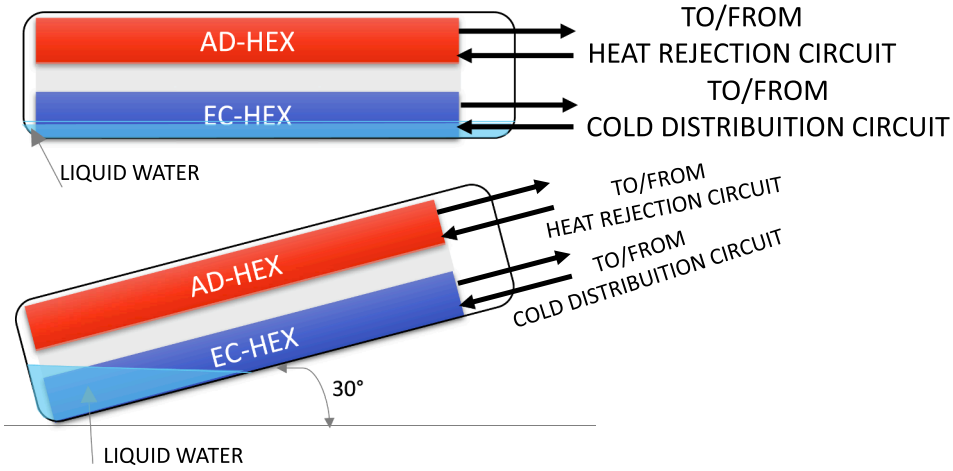

Fig. 13. Water level at the evaporator for 0° and 30° operation.

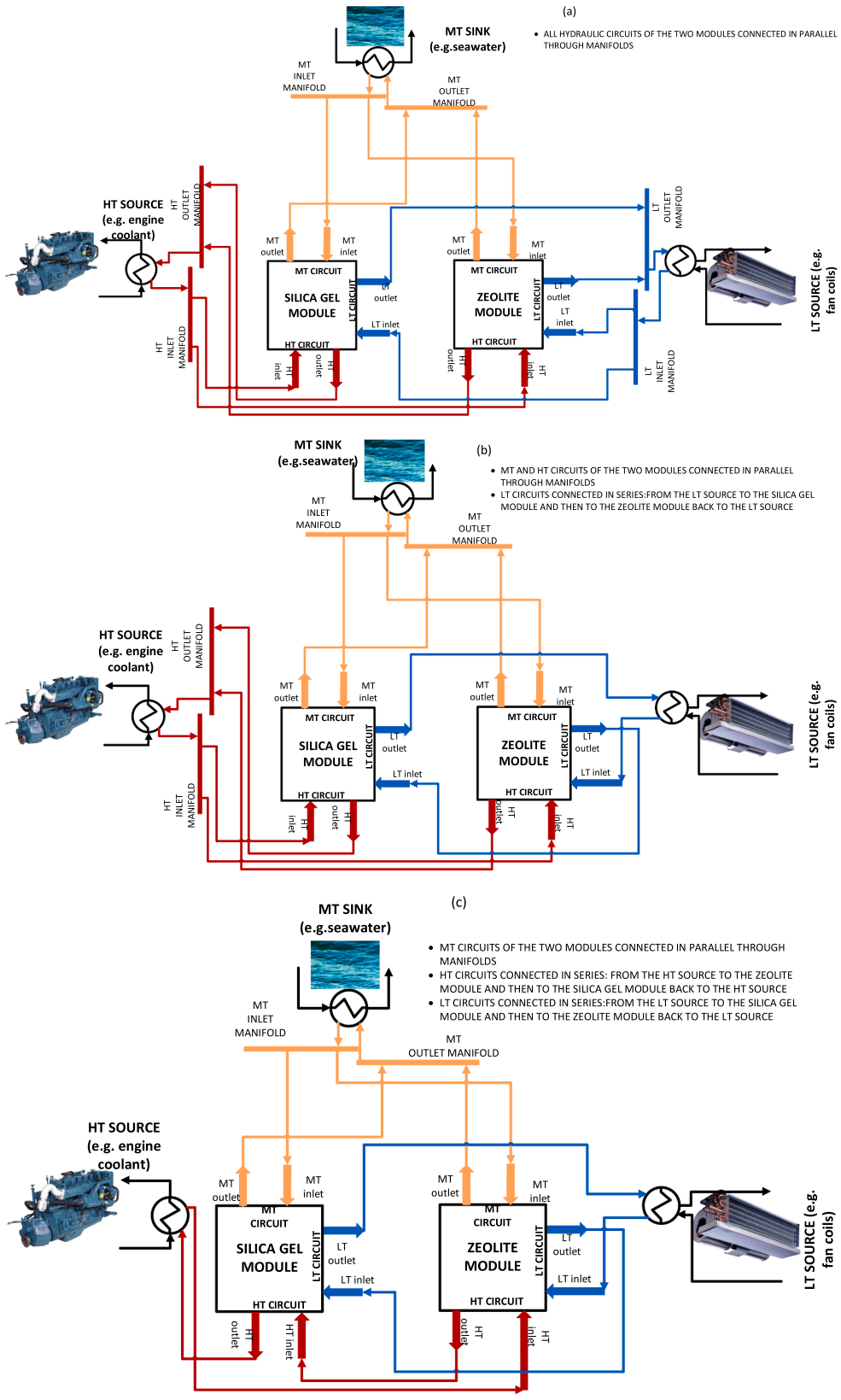

Fig. 14. The configurations for hybrid chiller evaluated.

previously mentioned, between the configurations (b) and (c), the configuration (c) is to be preferred, since it requires smaller pumps and pipes for the HT circuit.

9. Conclusions

The key aspect of the present work was the study of the effects of dynamic conditions due to wave motion on the operation of process

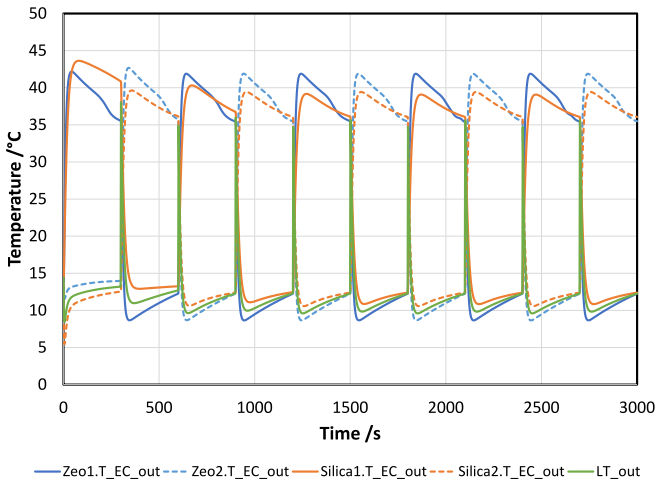

Fig. 15. Temperature trends for the evaporator-condenser in the hybrid configuration (a). Zeo1 and Silica1 modules are working in phase, Zeo2 and Silica2 modules are working in phase. LT_out is the overall outlet temperature on the cold distribution circuit.

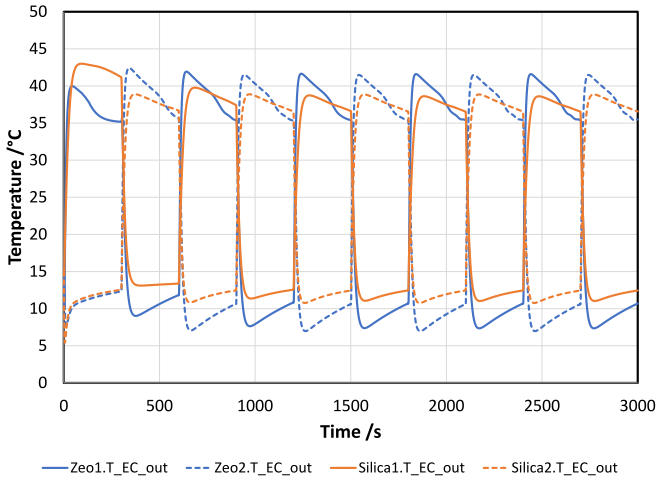

Fig. 16. Temperature trends for the evaporator-condenser in the hybrid configuration (b). Zeo1 and Silica1 modules are working in phase, Zeo2 and Silica2 modules are working in phase The LT outlet corresponds to the outlet temperature from Zeo1 and Zeo2.

modules for adsorption chillers (i.e. the couple of adsorber and evaporator/condenser). The simultaneous presence of the vapor phase and the liquid phase of the working fluid inside the circuit of the modules makes their operation sensitive to the inclinations caused by the motions of the ship. The tests were carried out by means of a lifting platform with hydraulic actuators with two degrees of freedom, considering permanent tilting and continuous movement, with different inclinations (from 10° to 30°), in order to reproduce rolling conditions that are even harsher than the operational case. Two different modules were tested, differing for the adsorbent material, silica gel and SAPO-34 zeolite.

In comparing the various scenarios, it emerged that the most severe operating condition for both modules is that of permanent inclination. The best performances were recorded with the modules arranged horizontally and with a heat sink circuit temperature of 27 °C. The maximum values of mean specific cooling power (SCP) were equal to 1.3 kW/kg for the module with zeolite and 0.6 kW/kg for the module with silica gel. The highest average powers, normalized with respect to the evaporator exchange surface, are equal to 7.4 kW/m^2 for the module with zeolite and 8.6 kW/m^2 for the module with silica gel.

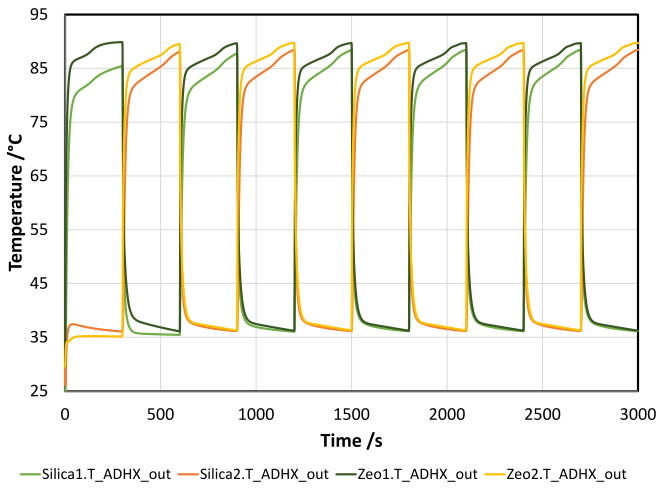

Fig. 17. Temperature trends for the adsorbers in the hybrid configuration (c). Zeo1 and Silica1 modules are working in phase, Zeo2 and Silica2 modules are working in phase The inlet of the Silica1 and Silica2 modules corresponds to the outlet of Zeo1 and Zeo2 modules.

The highest specific cooling energy (SCE) is 0.26 kWh/kg for the zeolite module and 0.18 kWh/kg for the silica gel module. The inclination resulted in a reduction of the cooling energy supplied by 22.5 % for the module with zeolite and by 55.8 % for the module with silica gel. The condition of movement, with the same heat transfer fluid flow rate, is associated with a reduction of the cooling energy of 21 % for the module with zeolite and of 29.1 % for the module with silica gel. By imposing a lower flow rate, the zeolite module subjected to movement recorded cooling energy values even higher than those achieved in a horizontal position. In conditions of oscillation higher cooling energy values were therefore recorded than in conditions of static inclination.

10. Future perspectives

In order to avoid oversizing the chiller to compensate for the lower performance when operating in tilted conditions, the strategy proposed was to foresee a chiller with modules with different materials within the same system. Three cases were evaluated in terms of serial or parallel connection of silica gel modules and zeolite modules and it was found out that the best case is a solution with parallel connection of MT circuits and serial connection of HT and LT circuits, with zeolite module as the topping module for the HT circuit and the silica gel module is the topping module for the LT circuit. This solution also allows to use the adsorption chiller efficiently even in the operating conditions of fan coil distribution systems. The experimental proof of this finding can further pave the way for the real and massive application of adsorption systems for the waste-to-cold conditions on board.

Ethical approval

This study does not contain any studies with human or animal subjects performed by any of the authors.

CRediT authorship contribution statement

Valeria Palomba: Writing – original draft, Visualization, Supervision, Software, Project administration, Investigation, Funding acquisition, Formal analysis, Data curation. **Antonino Bonanno:** Writing – original draft, Visualization, Methodology, Investigation, Formal analysis, Data curation, Conceptualization. **Vincenza Brancato:** Writing – review & editing, Validation, Investigation, Data curation. **Andrea Frazzica:** Writing – original draft, Visualization, Validation, Methodology, Investigation, Conceptualization. **Ralph Herrmann:** Writing –

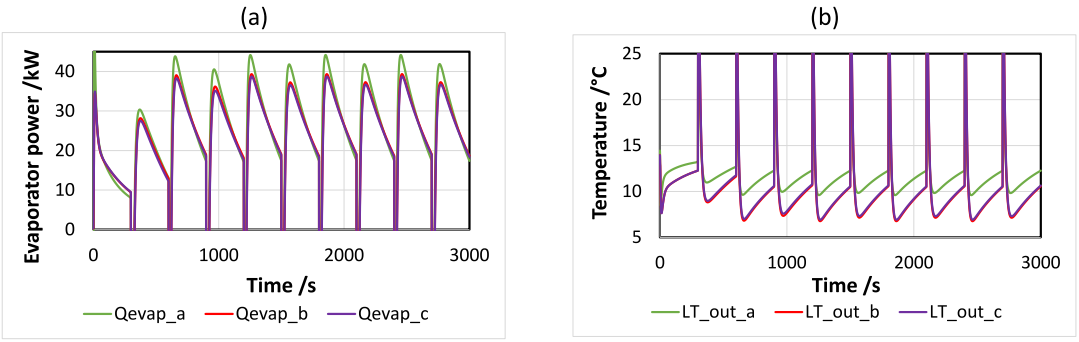

Fig. 18. Comparison of the simulated configurations in terms of (a) cooling power and (b) outlet temperature to user (evaporator) circuit.

review & editing, Supervision, Project administration, Funding acquisition, Formal analysis.

Declaration of competing interest

The authors declare that they have no known competing financial interests or personal relationships that could have appeared to influence the work reported in this paper.

Data availability

Data will be made available on request.

Acknowledgements

The present work is funded by the European Commission under the H2020 Framework under Grant Agreement 955413 (ENGIMMONIA).

Appendix A. Sensors and measurement of uncertainty

A list of installed sensors in the testing rig is reported in Table A.1.

Table A.1
Installed sensors.

Sensor	Accuracy	Measured parameter	Installation location
Type T thermocouples	Class A	Inlet and outlet temperature of all hydraulic circuits.	Testing rig
Magnetic flow meters MagView MVM-100-Q	± 1 % RD	Flow rates in all hydraulic circuits.	Testing rig
Type T thermocouples	Classe A	Inlet and outlet temperatures of the AdHEX and EC-HEX	Process module under testing
Edward ASG2-1000 capacitive pressure sensor	± 0,2% FS	Pressure inside the module	Process module under testing

Uncertainty analysis can be carried out according to the extended uncertainty theory. The uncertainty on thermal power can be defined as:

$$u(\dot{Q}) = \sqrt{\left[\frac{\delta \dot{Q}}{\delta \dot{m}} u(\dot{m})\right]^2 + \left[\frac{\delta \dot{Q}}{\delta \Delta T} u(\Delta T)\right]^2} \quad \text{(A1)}$$

where $u(\dot{m})$ and $u(\Delta T)$ were calculated for a triangular probability distribution as suggested by UNI CEI ENV 13005:

$$u(x) = \frac{a}{\sqrt{6}} \quad \text{(A2)}$$

For the flow measures, the "a" factor is indicated by the instrument provider and, in this case, is 1 % of measured value. For the class A Pt100m the value of a = 0.1 °C was used.

Considering the experimental results, the $u(\dot{Q})$ was estimated to be in the range of 6–8 %.

Appendix B. Model validation

The model was validated using data from experimental tests carried out at CNR; the tests on the Siogel module used for validation are those reported in [10], whereas the ones for the SAPO34 module are those reported in [22].

The numerical and experimental results for the SAPO34 are compared in terms of temperature profiles of adsorber, evaporator/condenser and COP, as shown in Figure A1.a-c. Generally, the experimental and simulated out temperature curves of both adsorber and evaporator/condenser are very close, with a temperature difference between the experiments and the simulations of 2.9 K on average.

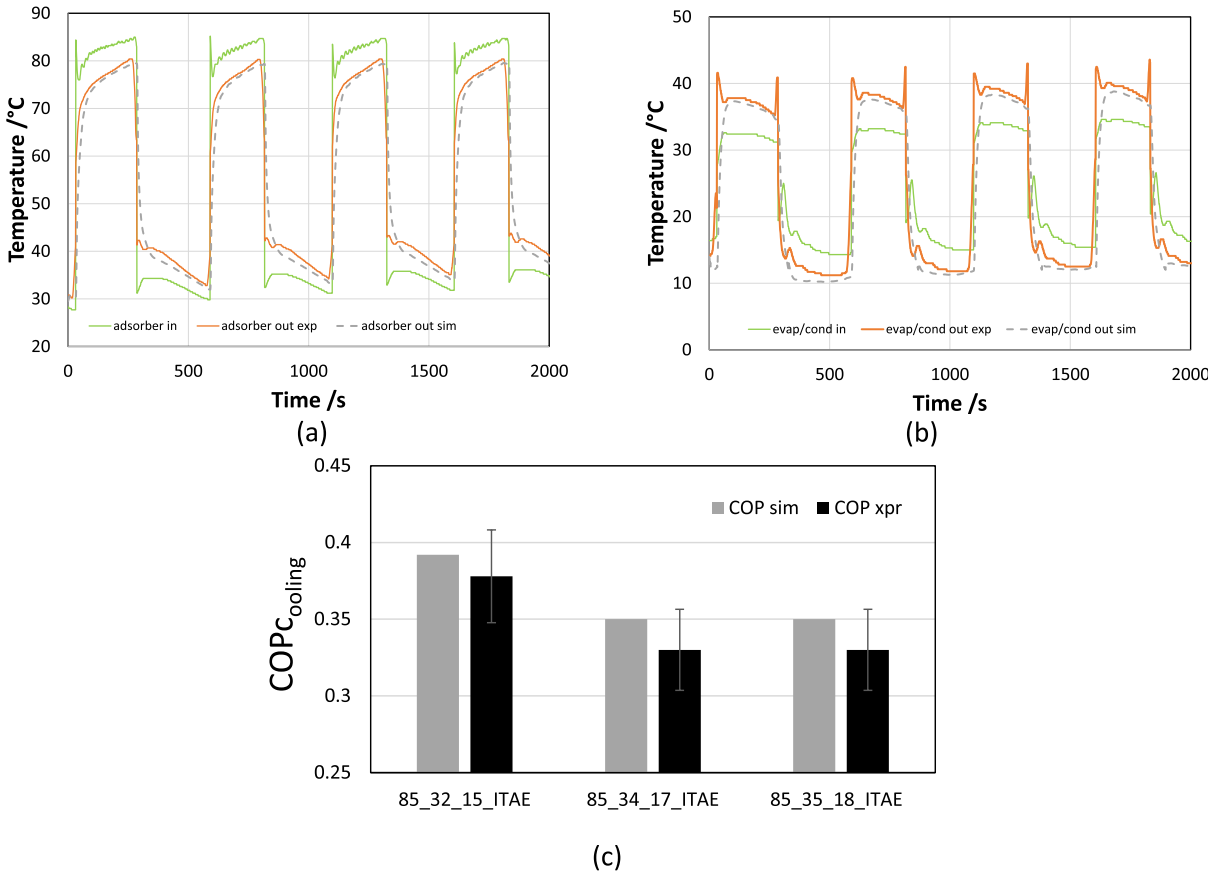

Fig. A.1. Comparisons of simulation and experimental evolutions of the temperature of (a) adsorber and (b) evaporator/condenser and (c) comparison of simulated and experimental COP for the SAPO34 module.

The results for the Siogel module are reported in. The average difference of simulated and experimental outlet temperature during desorption and evaporation is within 5 % which is the experimental uncertainty.

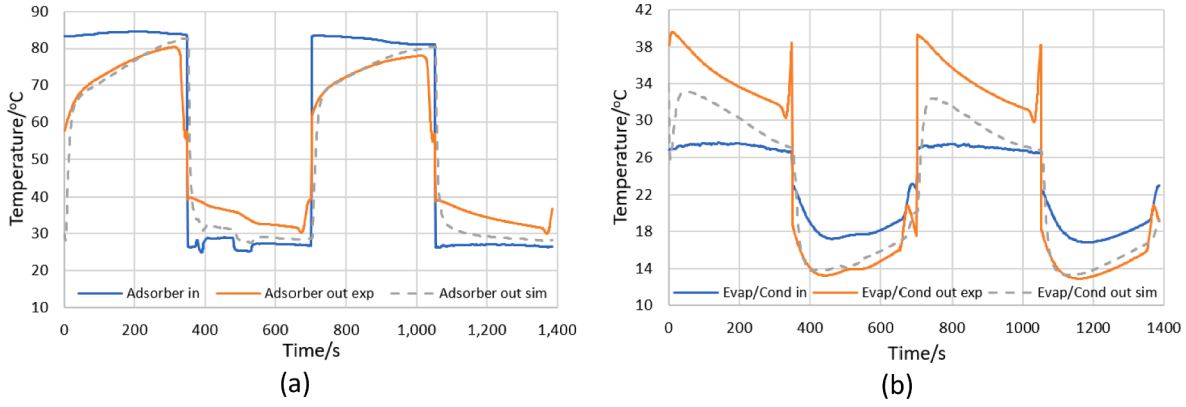

Fig. A.2. Comparisons of simulation and experimental evolutions of the temperature of (a) adsorber and (b) evaporator/condenser for the Siogel module.

The results here presented indicate that the implemented model is suitable to reproduce the behavior of the two process modules tested.

Appendix C. Supplementary data

Supplementary data to this article can be found online at https://doi.org/10.1016/j.applthermaleng.2024.123224.

References

[1] International Energy Agency. International Shipping - Tracking Report, 2022.
[2] D. Huang, Y. Wang, C. Yin, Selection of co_2 emission reduction measures affecting the maximum annual income of a container ship, J. Mar. Sci. Eng. 11 (2023) 534, https://doi.org/10.3390/JMSE11030534.
[3] C. Ononogbo, E.C. Nwosu, N.R. Nwakuba, G.N. Nwaji, O.C. Nwufo, O. C. Chukwuezie, et al., Opportunities of waste heat recovery from various sources: review of technologies and implementation, Heliyon (2023) 9, https://doi.org/10.1016/J.HELIYON.2023.E13590.

[4] S. Suárez de la Fuente, T. Cao, A.G. Pujol, A. Romagnoli, Waste heat recovery on ships. Sustainable Energy Systems on Ships: Novel Technologies for Low Carbon Shipping (2022) 123–95. Doi: 10.1016/B978-0-12-824471-5.00011-6.
[5] A.G. Olabi, K. Elsaid, M.K.H. Rabaia, A.A. Askalany, M.A. Abdelkareem, Waste heat-driven desalination systems: perspective, Energy 209 (2020) 118373, https://doi.org/10.1016/j.energy.2020.118373.
[6] V. Palomba, M. Aprile, M. Motta, S. Vasta, Study of sorption systems for application on low-emission fishing vessels, Energy 134 (2017) 554–565, https://doi.org/10.1016/j.energy.2017.06.079.
[7] Z. Lu, R. Wang, Experimental performance study of sorption refrigerators driven by waste gases from fishing vessels diesel engine, Appl. Energy 174 (2016) 224–231, https://doi.org/10.1016/J.APENERGY.2016.04.102.
[8] D. Butrymowicz, J. Gagan, M. Łukaszuk, K. Śmierciew, A. Pawluczuk, T. Zieliński, et al., Experimental validation of new approach for waste heat recovery from combustion engine for cooling and heating demands from combustion engine for maritime applications, J. Clean Prod. (2021) 290, https://doi.org/10.1016/J.JCLEPRO.2020.125206.
[9] S. Longo, V. Palomba, M. Beccali, M. Cellura, S. Vasta, Energy balance and life cycle assessment of small size residential solar heating and cooling systems equipped with adsorption chillers, Sol. Energy 158 (2017) 543–558.
[10] G.E. Dino, V. Palomba, E. Nowak, A. Frazzica, Experimental characterization of an innovative hybrid thermal-electric chiller for industrial cooling and refrigeration application, Appl. Energy (2021) 281, https://doi.org/10.1016/j.apenergy.2020.116098.
[11] D. Palomba, M. Ghirlando, Frazzica, Decarbonising the shipping sector: a critical analysis on the application of waste heat for refrigeration in fishing vessels, Appl. Sci. 9 (2019) 5143, https://doi.org/10.3390/app9235143.
[12] X. Xu, Y. Li, S. Yang, G. Chen, A review of fishing vessel refrigeration systems driven by exhaust heat from engines, Appl. Energy 203 (2017) 657–676, https://doi.org/10.1016/J.APENERGY.2017.06.019.
[13] R.Z. Wang, Efficient adsorption refrigerators integrated with heat pipes, Appl. Therm. Eng. 28 (2008) 317–326, https://doi.org/10.1016/j.applthermaleng.2006.02.028.
[14] V. Palomba, B. Dawoud, A. Sapienza, S. Vasta, A. Frazzica, On the impact of different management strategies on the performance of a two-bed activated carbon/ethanol refrigerator: an experimental study, Energy Convers. Manag. 142 (2017) 322–333, https://doi.org/10.1016/j.enconman.2017.03.055.
[15] F. Baldi, F. Ahlgren, T.-V. Nguyen, M. Thern, K. Andersson, Energy and exergy analysis of a cruise ship, Energies (Basel) 11 (2018) 2508, https://doi.org/10.3390/en11102508.
[16] M.A. Ancona, F. Baldi, M. Bianchi, L. Branchini, F. Melino, A. Peretto, et al., Efficiency improvement on a cruise ship: Load allocation optimization, Energy Convers. Manag. 164 (2018) 42–58, https://doi.org/10.1016/j.enconman.2018.02.080.
[17] D. Dadpour, M. Deymi-Dashtebayaz, A. Hoseini-Modaghegh, M. Abbaszadeh-Bajgiran, S. Soltaniyan, E. Tayyeban, Proposing a new method for waste heat recovery from the internal combustion engine for the double-effect direct-fired absorption chiller, Appl. Therm. Eng. (2022) 216, https://doi.org/10.1016/j.applthermaleng.2022.119114.
[18] W. Salmi, J. Vanttola, M. Elg, M. Kuosa, R. Lahdelma, Using waste heat of ship as energy source for an absorption refrigeration system, Appl. Therm. Eng. 115 (2017) 501–516, https://doi.org/10.1016/J.APPLTHERMALENG.2016.12.131.
[19] Y. Son, S. Lee, S. Heo, Evaluation of the ship motion effects on the NaOH/air absorption system performance, Chem. Eng. Sci. 207 (2019) 1049–1059, https://doi.org/10.1016/j.ces.2019.07.028.
[20] V. Palomba, S. Nowak, B. Dawoud, A. Frazzica, Dynamic modelling of adsorption systems: a comprehensive calibrateddataset for heat pump and storage applications, J. Energy Storage 33 (2021) 102148, https://doi.org/10.1016/j.est.2020.102148.
[21] V. Brancato, A. Frazzica, Characterisation and comparative analysis of zeotype water adsorbents for heat transformation applications, Sol. Energy Mater. Sol. Cells 180 (2018) 91–102, https://doi.org/10.1016/J.SOLMAT.2018.02.035.
[22] V. Palomba, A. Bonanno, G. Brunaccini, D. Aloisio, F. Sergi, G.E. Dino, et al., Hybrid cascade heat pump and thermal-electric energy storage system for residential buildings: experimental testing and performance analysis, Energies (Basel) 14 (2021) 2580, https://doi.org/10.3390/en14092580.
[23] F. Lanzerath, J. Seiler, M. Erdogan, H. Schreiber, M. Steinhilber, A. Bardow, The impact of filling level resolved: Capillary-assisted evaporation of water for adsorption heat pumps 2016, doi: 10.1016/j.applthermaleng.2016.03.052.
[24] V. Palomba, A. Frazzica, Experimental study of a fin-and-tube heat exchanger working as evaporator in subatmospheric conditions, Appl. Therm. Eng. 175 (2020) 115336, https://doi.org/10.1016/j.applthermaleng.2020.115336.
[25] R. Volmer, J. Eckert, G. Füldner, L. Schnabel, Evaporator development for adsorption heat transformation devices – influencing factors on non-stationary evaporation with tube-fin heat exchangers at sub-atmospheric pressure, Renew. Energy 110 (2017) 141–153, https://doi.org/10.1016/J.RENENE.2016.08.030.
[26] V. Palomba, W. Lombardo, A. Groβe, R. Herrmann, B. Nitsch, A. Strehlow, et al., Evaluation of in-situ coated porous structures for hybrid heat pumps, Energy 209 (2020) 118313, https://doi.org/10.1016/j.energy.2020.118313.
[27] V. Palomba, G.E. Dino, A. Frazzica, Coupling sorption and compression chillers in hybrid cascade layout for efficient exploitation of renewables: sizing, design and optimization, Renew. Energy 154 (2020) 11–28, https://doi.org/10.1016/J.RENENE.2020.02.113.
[28] DNV. DNVGLCG0339 - Environmental test specification forelectrical, electronic and programmableequipment and systems, 2019.
[29] J. Seiler, R. Volmer, D. Krakau, J. Pöhls, F. Ossenkopp, L. Schnabel, et al., Capillary-assisted evaporation of water from finned tubes – impacts of experimental setups and dynamics, Appl. Therm. Eng. 165 (2020) 114620, https://doi.org/10.1016/J.APPLTHERMALENG.2019.114620.
[30] A. Sapienza, V. Palomba, G. Gullì, A. Frazzica, S. Vasta, A new management strategy based on the reallocation of ads-/desorption times: Experimental operation of a full-scale 3 beds adsorption chiller, Appl. Energy 205 (2017) 1081–1090, https://doi.org/10.1016/J.APENERGY.2017.08.036.
[31] A. Gibelhaus, T. Tangkrachang, U. Bau, J. Seiler, Integrated design and control of full sorption chiller systems, Energy 185 (2019) 409–422, https://doi.org/10.1016/j.energy.2019.06.169.
[32] S.H. Seol, K. Nagano, J. Togawa, Modeling of adsorption heat pump system based on experimental estimation of heat and mass transfer coefficients, Appl. Therm. Eng. 171 (2020) 115089, https://doi.org/10.1016/J.APPLTHERMALENG.2020.115089.
[33] M.J. Rupa, A. Pal, S. Mitra, B.B. Saha, Time adapted linear driving force model for gas adsorption onto solids, Chem. Eng. J. 420 (2021) 129785, https://doi.org/10.1016/J.CEJ.2021.129785.
[34] A. Velte, G. Füldner, E. Laurenz, L. Schnabel, Advanced measurement and simulation procedure for the identification of heat and mass transfer parameters in dynamic adsorption experiments, Energies (Basel) (2017) 10, https://doi.org/10.3390/en10081130.
[35] V. Palomba, E. Varvagiannis, S. Karellas, A. Frazzica, Hybrid adsorption-compression systems for air conditioning in efficient buildings: design through validated dynamic models, Energies (Basel) 12 (2019) 1161, https://doi.org/10.3390/en12061161.